

Near-infrared intersubband transitions in delta-doped InAs/AlSb multi-quantum wells

S. Sasa,^{a)} Y. Nakajima, M. Nakai, and M. Inoue

New Materials Research Center, Osaka Institute of Technology, 5-16-1 Ohmiya Asahi-ku, Osaka 535-8585, Japan

D. C. Larrabee and J. Kono

Department of Electrical and Computer Engineering, Rice Quantum Institute, and Center for Nanoscale Science and Technology, Rice University, Houston, Texas 77005

(Received 26 August 2004; accepted 16 October 2004)

Intersubband transitions (ISBTs) in narrow InAs/AlSb multiple quantum wells (MQWs) were investigated for well widths, d , ranging from 5 nm down to 1.8 nm with 10, 20, or 60 periods. In order to observe a strong ISBT signal, a heavy silicon doping was made in each InAs quantum well. Delta doping was employed for the narrowest wells to prevent silicon incorporation into the AlSb barrier layers. As the well width decreased, the ISBT signal of the MQWs decreased. However, it persisted down to $d=2.1$ nm with a sheet doping density in each quantum well of $9 \times 10^{12} \text{ cm}^{-2}$ and 60 periods. The ISBT signal observed for $d=2.1$ nm was peaked at an energy of 650 and 670 meV at 300 and 77 K, respectively. These are the highest energy values ever observed for ISBTs in InAs/AlSb MQWs. © 2004 American Institute of Physics. [DOI: 10.1063/1.1833559]

The 6.1 Å group of semiconductors (GaSb, InAs, and AlSb) is a system for applications in both infrared optoelectronics¹ and high-speed and low power-consumption electronics.² For example, high-speed all-optical switches and modulators are possible applications relying on the extremely short intersubband relaxation times. Because of the large conduction band discontinuity between InAs and AlSb (~ 2.1 eV), the 6.1 Å group offers greater flexibility in designing intersubband optical devices operating at a shorter wavelength range compared to the well-developed GaAs/AlGaAs system. For applications to optical communications, operations in the near-infrared (NIR) region such as 1.55 μm (0.80 eV) are desirable. Operations at this wavelength are also advantageous for the realization of all optical THz sources pumped by a compact NIR diode laser.³

Due to the small effective mass in InAs, the oscillator strength for intersubband transitions (ISBTs) is strong. This allows one to observe the NIR ISBT in InAs/AlSb quantum wells (QWs) with a small number of periods, such as 10. For comparison, in higher-mass systems such as GaN/AlN (Ref. 4) or InGaAs,^{5,6} as many as 100 QWs may be required to observe the NIR ISBT easily. In addition, the smaller effective mass allows a wider well width to be used for the same operating wavelength compared to other material systems. This reduces broadening of the ISBT, which is primarily caused by monolayer fluctuations at the interface, and allows greater flexibility in the design of the QW.

We study the well width dependence of the intersubband transitions (ISBTs) in heavily doped InAs/AlSb multiple quantum wells (MQWs) with 10, 20, or 60 periods and report that near-infrared (NIR) absorption can be obtained in narrow quantum wells. In our previous reports,⁷ the InAs quantum well layers were unintentionally doped. The MQWs, however, showed n-type conduction with a total sheet electron density of the order of 10^{12} cm^{-2} . The ISBT energy increased as the well width decreased and the absorp-

tion disappeared for $d < 5$ nm. The absorption coefficient obtained by a simple model is inversely proportional to the effective mass.⁸ Owing to the strong nonparabolicity in InAs, the ISBT signal thus decreases as the well width decreases. Recently, Ohtani *et al.* have reported ISBTs in doped InAs/AlSb QWs as narrow as 2.7 nm (Ref. 9) demonstrating the advantageous feature of this material system for optical devices utilizing ISBTs in NIR region. Here, we explored narrower InAs/AlSb MQWs with a relatively small number of periods compared to these previous reports in order to obtain ISBTs in the NIR region.

The InAs/AlSb MQWs were prepared by molecular beam epitaxy. The structure is grown on a (100) semi-insulating GaAs substrate. In order to accommodate the lattice mismatch between the MQW layer and GaAs substrate, a 300-nm-thick GaSb layer, a 1-μm-thick AlSb layer, 15 periods of GaSb (6 nm)/AlSb (6 nm) superlattice layers, and a 200-nm-thick AlGaSb layer were grown as the buffer layer. On top of the buffer layer, 20 periods of Si-adopted InAs/AlSb MQWs were grown at a substrate temperature of 420 °C. The MQW is composed of InAs quantum wells with various thicknesses and AlSb barrier layers. The InAs well width, d , was varied from 5 nm down to 1.8 nm, while the AlSb barrier layers were kept constant at 10 nm. The hetero-interface between InAs and AlSb was controlled by the shutter sequence to be InSb bonds. Finally, a 5-nm-thick InAs cap layer was grown to pin the surface Fermi energy at about the same energy above the InAs conduction band as the Fermi energy deep in the MQWs. This ensures a uniform distribution of electrons through the MQW structure.¹⁰ Since the ISBT intensity is proportional to the total electron density in the structure, a heavy doping with Si was made in each InAs QW layer. For $d \geq 2.7$ nm a 1-nm-thick InAs setback layer was formed at each side of the doped region in order to eliminate dopant incorporation into the AlSb barrier, in which a Si atom becomes an acceptor. The central part of the InAs was uniformly doped. In order to keep the sheet doping density constant, the Si-cell temperature was adjusted de-

^{a)}Electronic mail: sasa@ee.oit.ac.jp

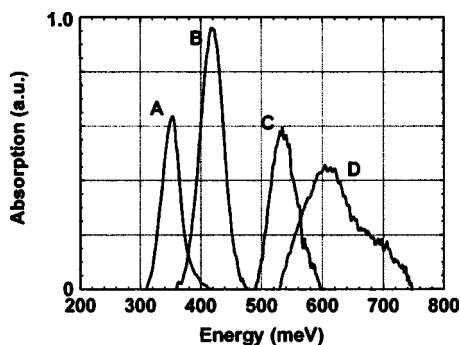


FIG. 1. Intersubband absorption spectra of InAs/AlSb MQWs at 79 K for samples A, B, C, and D. A large line width broadening is observed for sample D.

pending on the well thickness. The sheet electron density in each QW is about $2\text{--}3 \times 10^{12} \text{ cm}^{-2}$. Therefore, the total concentration was a few $\times 10^{13} \text{ cm}^{-2}$ regardless of the well width. The sample structures were characterized by x-ray diffraction and intersubband absorption measurements.

The ISBT was measured with a Fourier transform infrared spectrometer as described in Ref. 7. The sample was processed in a multibounce geometry and the ratio of the transmission of *p*- and *s*- polarized light (ISBT active and inactive) was measured. The background was the *p/s* ratio with no sample. The absorption coefficient is $-\ln(\text{transmission ratio})$, normalized by the size of the sample and the number of QWs. Figure 1 shows the absorption signals measured at 77 K for the MQW structures, $d=5.0, 4.0, 3.0,$ and 2.7 nm (samples A–D). Table I summarizes the sample structure and total sheet electron density measured by van der Pauw method at 77 K. The period of MQW is 20 except for sample D (2.7 nm), which has ten periods. In order to keep the total density constant, the sheet doping density per well was doubled for sample D. A strong absorption due to ISBT is observed for all the structures, although the number of InAs QW layers is relatively small. This is an advantageous feature of InAs-based MQWs for applications to all-optical devices. The highest peak energy obtained for this set of samples is 620 meV in sample D, which is somewhat lower in energy than the previous report by Ohtani *et al.*⁹ A large line width broadening is also observed for sample D while a gradual increase in the line width is observed for samples between A and C. The reason for the large line width broadening for sample D will be discussed later.

It is known that the mobility exhibits an L^6 dependence on the well width, d for $d < 5 \text{ nm}$.^{11,12} Interface roughness at

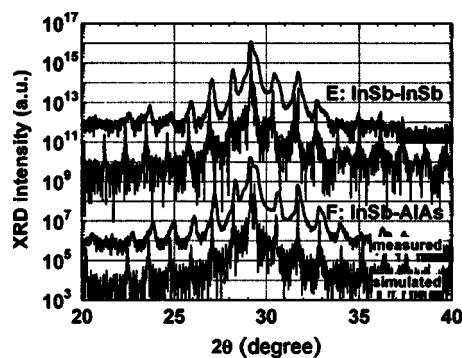


FIG. 2. Measured and simulated XRD spectra for two types of InAs (1.8 nm)/AlSb (5.4 nm) MQWs. The top two curves are of MQW with InSb bonds at each interface (sample E) and the lower for MQW with InSb top and AlAs bottom interfaces (sample F).

each heterointerface is considered to be critical for the ISBT line width for this range of d .^{13,14} In order to check the structural quality of the MQW structure including the interface layer, we grew two types of MQW structures, one with InSb bonds for both heterointerfaces (sample E) and the other with InSb at the top interface and AlAs at the bottom interface in the well (sample F). The thicknesses of InAs and AlSb were 1.8 and 5.4 nm, respectively. The MQWs were grown on top of a thick AlSb buffer layer. X-ray diffraction (XRD) spectra for the two types of MQW is shown in Fig. 2 together with simulated XRD spectra for each MQW. In this MQW structure, the layer thicknesses were designed so that the XRD peak of the MQW structure is at the same angle as the bulk AlSb peak when InSb interfaces, i.e., 1-ML-thick InSb interlayers, are formed at both interfaces. As can be seen in the figure, the zero-order MQW peak coincides to that of AlSb for sample E, while distinct peaks for the MQW and AlSb are clearly observed for sample F. This means that the MQW structures including the interface layers of either InSb or AlAs are grown in a well controlled fashion even for such narrow InAs QWs. The structural integrity of the samples for the ISBT measurements was confirmed in the same manner.

In order to study the well width dependence of the ISBT intensity, we estimated the integrated absorption intensity for spectra shown in Fig. 1. For the development of optical devices, the integrated absorption intensity as well as the peak intensity is important. The integrated intensity was divided by the sheet doping density for normalization and is shown in Fig. 3. There is a rapid reduction in the integrated intensity for d between 2 and 3 nm. This behavior cannot be well explained by a simple model. However, the model also indi-

TABLE I. Sample structure, electron density, and mobility at 77 K in MQWs.

Sample	Well width, d (nm)	Setback layer (nm)	Period	Total density (cm^{-2})	Mobility ($\text{cm}^2/\text{V s}$)
A	5.0	1	20	4.2×10^{13}	4150
B	4.0	1	20	5.8×10^{13}	2490
C	3.0	1	20	5.6×10^{13}	1190
D	2.7	1	10	6.0×10^{13}	1720
E	1.8	-	-	-	-
F	1.8	-	-	-	-
G	2.1	1.05	20	2.9×10^{14}	414
H	1.8	0.9	20	2.2×10^{14}	360
I	2.1	1.05	60	5.5×10^{14}	209

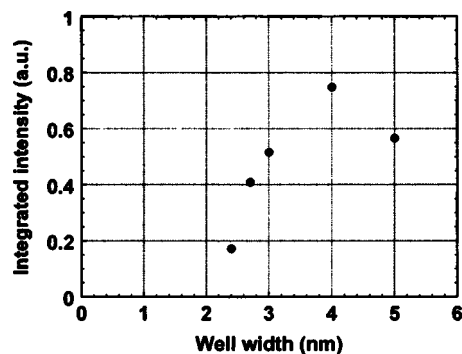


FIG. 3. Integrated ISBT intensity for samples A–D. A drastic reduction in the intensity occurs for d between 2 and 3 nm.

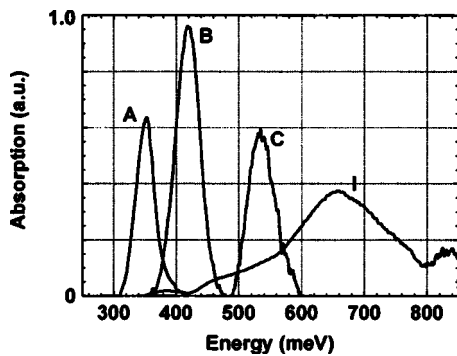


FIG. 4. Intersubband absorption spectrum for 60 periods of MQW with $d = 2.1$ nm (sample I) together with those for samples A, B, and C.

icates that both the sheet doping density and period of MQW contribute to the ISBT. A higher doping would lead to multiple-subband occupation. This would reduce the intensity of the lowest energy ISBT due to state filling but, the higher energy ISBT would have a large ISBT intensity since the oscillator strength in higher subband is much stronger. Intersubband transitions in near-infrared region are indeed reported taking advantage of the ISBT among higher subbands in InGaAs/AlAs MQWs.⁸ In the next set of samples, we increased the doping density per well and the MQW period in order to strengthen the ISBT intensity.

Next, we grew three MQW samples G, H, and I with a higher doping density of about $1 \times 10^{13} \text{ cm}^{-2}$ per well using a Si delta doping. The well width, d , was 2.1 nm for samples G and I and 1.8 nm for sample H. The delta doping was made at the center of the QW. Note that a 3-ML-thick InAs setback layer still exists in sample H. The doping density was increased by a factor of 3–4 compared to that of samples A–D by the use of the delta doping. The period of the MQW was 20 for samples G and H and 60 for sample I. For sample I, both the doping density and MQW period were increased. Figure 4 shows the 77 K ISBT spectrum of sample I together with those for samples A, B, and C. No ISBT signal was observed for samples G and H despite the high doping density. As can be seen, a strong absorption accompanied by a large line width broadening was observed for sample I. The small shoulder around 700 meV is due to Fabry–Perot interference. The peak energy of sample I was 670 meV at 77 K and 650 meV at R.T. These are the highest ISBT energies observed in InAs/AlSb MQWs. The observation of NIR ISBTs in so few MQW periods demonstrates the material feasibility of InAs/AlSb system for the development of intersubband devices, such as a THz light source.

As shown in Table I, the samples which exhibited a large linewidth broadening showed a large mobility reduction compared to that in wider wells such as sample A. In order to measure the low mobility values, the InAs cap layer was selectively removed to eliminate the contribution from the cap layer. We found that the mobility shows a d^6 dependence for d below 3 nm at 77 K. We examined several MQW structures to confirm the dependence although the MQWs are not shown in Table I unless the absorption measurements

were carried out. We also found that subband energy fluctuation due to 1 ML fluctuation of the well thickness is not enough to explain the broadening. However, the mean free time obtained from the mobility explains the ISBT linewidth for the narrowest MQWs. The mobility value of $209 \text{ cm}^2/\text{Vs}$ (sample I) corresponds to the linewidth of 0.2 eV. Therefore, roughness scattering dominates the ISBT linewidth for narrowest wells as is previously reported.^{13,14} In Ref. 14, it is also reported that the ISBT linewidth is dominated by interface roughness scattering while the mobility is much less sensitive to the interface roughness. The reason for the good quantitative agreement in our case is not clear at present. One possibility is that the doping scheme of the two cases, doped well for this work and modulation doping for Ref. 14.

In conclusion, we studied the well width dependence of the ISBTs in heavily doped InAs/AlSb MQWs. An ISBT energy of 670 meV was obtained for $d = 2.1$ nm at 77 K, which is the highest energy ISBT in this material system. Our results indicate that the increasing the number of MQW periods is more effective than increasing the doping density in the well for increasing the ISBT intensity. The linewidth is governed by the scattering time due to interface roughness for the narrowest ($d < 3$ nm) MQWs.

The authors are grateful to G. G. Walden for sample preparation and A. J. Rimberg for the use of his evaporator. This work is partly supported by DARPA/AFOSR F49620-01-10543, NASA-NCIBSRP, and the Robert A. Welch Foundation.

¹J. L. Bradshaw, R. Q. Yang, J. D. Bruno, J. T. Pham, and D. E. Wortman, *Appl. Phys. Lett.* **75**, 2362 (1999).

²Y. Royter, K. R. Elliott, P. W. Deelman, R. D. Rajavel, D. H. Chow, I. Milosavljevic, and C. H. Fields, *IEEE Tech. Dig.* **IEEE-03**, 731 (2003).

³A. Liu and C. Z. Ning, *Appl. Phys. Lett.* **76**, 1984 (2000).

⁴K. Kishino, A. Kikuchi, H. Kanazawa, and T. Tachibana, *Appl. Phys. Lett.* **81**, 1234 (2002).

⁵T. Asano, S. Noda, T. Abe, and A. Sasaki *Jpn. J. Appl. Phys., Part 1* **35**, 1285 (1996).

⁶B. Sung, H. C. Chui, M. M. Fejer, and J. S. Harris, Jr., *Electron. Lett.* **33**, 818 (1997).

⁷D. C. Larrabee, G. A. Khodaparast, J. Kono, K. Ueda, Y. Nakajima, M. Nakai, S. Sasa, M. Inoue, K. I. Kolokolov, J. Li, and C. Z. Ning, *Appl. Phys. Lett.* **83**, 3936 (2003); D. C. Larrabee, J. Tang, M. Liang, G. A. Khodaparast, J. Kono, K. Ueda, Y. Nakajima, O. Suekane, S. Sasa, M. Inoue, K. I. Kolokolov, J. Li, and C. Z. Ning, *Proceedings of the 26th International Conference on Physics of Semiconductors*, edited by A. R. Long and J. H. Davies (Institute of Physics, Bristol, 2003), p. 129.

⁸See, for example, *Quantum Wells: Physics and Device Applications I & II*, edited by H. C. Liu and F. Capasso (Academic, New York, 2000).

⁹K. Ohtani and H. Ohno, *Appl. Phys. Lett.* **82**, 1003 (2003).

¹⁰C. Nguyen, B. Brar, and H. Kroemer, *J. Vac. Sci. Technol. B* **11**, 1706 (1993).

¹¹H. Sakaki, T. Noda, K. Hirakawa, M. Tanaka, and T. Matsusue, *Appl. Phys. Lett.* **51**, 1934 (1987).

¹²C. R. Bolognesi, H. Kroemer, and J. English, *J. Vac. Sci. Technol. B* **10**, 877 (1992).

¹³K. L. Campman, H. Schmidt, A. Imamoglu, and A. C. Gossard, *Appl. Phys. Lett.* **69**, 2554 (1996).

¹⁴T. Unuma, T. Takahashi, T. Noda, M. Yoshita, H. Sakaki, M. Baba, and H. Akiyama, *Appl. Phys. Lett.* **78**, 3448 (2001).